ACS APPLIED MATERIALS & INTERFACES

www.acsami.org

Research Article

Mechanically Interlocked Carbon Nanotubes as a Stable Electrocatalytic Platform for Oxygen Reduction

Dominik Wielend,[‖] Mariano Vera-Hidalgo,[‖] Hathaichanok Seelajaroen, Niyazi Serdar Sariciftci, Emilio M. Pérez,* and Dong Ryeol Whang*

Cite This: *ACS Appl. Mater. Interfaces* 2020, 12, 32615–32621

Read Online

ACCESS | Metrics & More | Article Recommendations | Supporting Information

ABSTRACT: Mechanically interlocking redox-active anthraquinone onto single-walled carbon nanotubes (AQ-MINT) gives a new and advanced example of a noncovalent architecture for an electrochemical platform. Electrochemical studies of AQ-MINT as an electrode reveal enhanced electrochemical stability in both aqueous and organic solvents compared to physisorbed AQ-based electrodes. While maintaining the electrochemical properties of the parent anthraquinone molecules, we observe a stable oxygen reduction reaction to hydrogen peroxide (H_2O_2). Using such AQ-MINT electrodes, 7 and 2 μmol of H_2O_2 are produced over 8 h under basic and neutral conditions, while the control system of SWCNTs produces 2.2 and 0.5 μmol, respectively. These results reveal the potential of this rotaxane-type immobilization approach for heterogenized electrocatalysis.

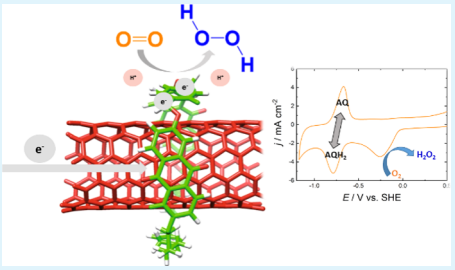

KEYWORDS: *electrocatalysis, oxygen reduction, immobilization, non-covalent architecture, rotaxane, hydrogen peroxide production*

1. INTRODUCTION

Great effort has been made worldwide on investigations of appropriate electrocatalysts for energy storage stategies such as batteries,[1−3] supercapacitors,[4] electrolysis of water,[5,6] and/or recycling of carbon dioxide (CO_2).[5,7−9] Due to their high efficiency, noble and rare metals, like platinum, palladium, and rhenium, serve as state-of-the-art electrocatalysts for various energy storage reactions, for example, reduction of protons,[10,11] CO_2,[12] and oxygen (O_2).[13−15] However, as these metals are costly, one approach is to substitute these metals with inexpensive and more abundant metals like nickel,[16] iron,[17] and manganese[18] or to use fully metal-free systems.[19] Especially regarding the oxygen reduction reaction (ORR), numerous reports on organic catalysts[20] and even small molecules[21] can be found in the literature.[13] Among those, anthraquinone (AQ) and its derivatives have been explored as molecular electrocatalysts for the ORR, since AQ is low-cost,[22] has suitable chemical functionality,[23] and high selectivity for H_2O_2.[24,25] Since physical deposition of AQ derivatives on electrodes suffered from low stability and slow reaction kinetics,[24] for long-term applications, immobilization and stabilization of the molecules at the electrode is of crucial importance.

To overcome this issue, various attempts were introduced, like covalently linking to glassy carbon (GC) electrodes,[26] using insoluble polymers,[27] or covalently linking to carbon nanotubes (CNTs).[28] Regarding a broader scope in organic electronics, organic molecules like AQ were also investigated in battery research[2,29,30] as well as in noncovalent enzyme-linking immobilization.[31]

CNTs are favorable immobilization platforms due to their attractive properties of being mechanically robust and having high electrical conductivity and tunability upon synthesis.[13,32] There are examples of antioxidant-linked CNTs in polymer additives,[33] and as they are supposed to be biocompatible,[31] CNTs are also employed in medical applications.[34] Park et al.[30] investigated nanohybrids of organic molecules adsorbed onto single-walled carbon nanotubes (SWCNTs) for battery application and reported significant improvement of electrical and electrochemical properties. Gong et al.[35] investigated similar adsorbed AQ on multiwalled CNTs (MWCNTs) for the electrochemical ORR in neutral solution. However, the direct covalent modification of CNTs is avoided. In general, SWCNTs have more uniform shapes and properties,[36] but their electrical conductivities are lower upon covalent modification compared to MWCNTs.[37] Combining both, high conductivity by noncovalent binding to the SWCNTs and still achieving close catalytic sites, Pérez et al. developed an advanced noncovalent rotaxane system wrapped around SWCNTs.[38−40] Recent studies from the Pérez group[41] inspired us to test those molecules for electrocatalytic application. In general, noncovalent architectures toward supramolecular molecular machines are of high interest in the scientific

Received: April 9, 2020
Accepted: June 23, 2020
Published: June 23, 2020

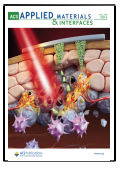

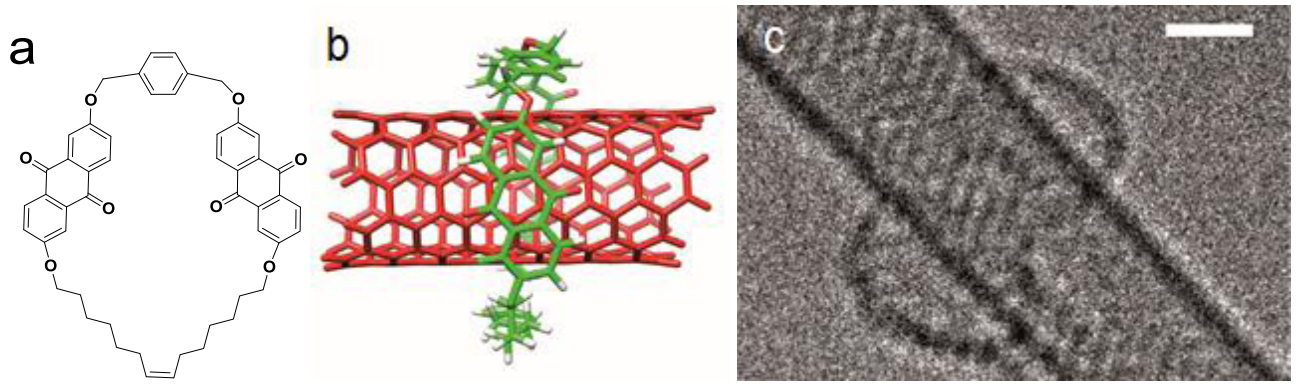

Figure 1. (a) Chemical structure of AQ-MINT, (b) minimum-energy geometry of AQ-MINT determined by DFT, and (c) the HR-TEM image of AQ-MINT (scale bar = 0.5 nm). (b and c) are adapted from Blanco et al.[41]

community due to the Nobel Prizes in 1987 for Cram, Lehn, and Pederson,[42] as well as recently in 2016 for Sauvage, Stoddart, and Feringa.[43−45]

The main objective of this work has two aspects: the first task was to investigate the electrochemical behaviors of a mechanically interlocked anthraquinone on SWCNTs (AQ-MINT) and compared it with an adsorbed anthraquinone (AQ) analogue (simple supramolecular form, AQ@SWCNTs) as well as with pure homogeneous AQ analogue cases. To do so, the properties of AQ as redox-active species on CNTs in aqueous solution and in organic solvents were compared with the properties of adsorbed and pure AQ cases, similar to reports on metal complexes.[46,47] The second task was to demonstrate the application of this immobilized AQ platform as an electrocatalyst for the ORR to H_2O_2.

2. EXPERIMENTAL SECTION

2.1. Characterization Methods. Thermogravimetric analyses (TGA) were performed using a TA Instruments TGA Q500 with a ramp of 10 °C min^{-1} under air from 100 to 900 °C. Raman spectra were acquired with a Bruker Senterra confocal Raman microscope instrument equipped with a 532 nm excitation laser. UV−vis−NIR spectra were obtained using an Agilent Technologies equipment—Cary Series UV−vis−NIR spectrophotometer. Photoluminescence excitation (PLE) intensity maps were obtained with a NanoLog 4 HORIBA instrument.

2.2. Synthesis of AQ-MINT. All chemicals were purchased and used as received, unless reported otherwise. The synthesis and characterization of macrocycle-AQ (mac-AQ)[48] and AQ-MINT[41] were done following previously reported procedures[49,50] (see Supporting Information Figures S1−S4 for further details). The structures of mac-AQ and AQ-MINT are shown in Figure 1. Figure 1 shows the optimized geometry structure (b) as well as a characteristic aberration-corrected high-resolution transmission electron microscopy (HR-TEM) image (c).

After the MINT-forming reaction, the SWCNTs showed a loading of the macrocycle of 13% and 15% under a nitrogen atmosphere for AQ-MINT and AQ@SWCNTs, respectively, by TGA analysis (Figure S5, S6). We also synthesized AQ-MINT and AQ@SWCNT samples with a low loading of the macrocycle to see the effect of anthraquinone content (Figures S5, S6). In the case of the low-loading synthesis of AQ-MINT and AQ@SWCNTs, the weight losses corresponding to the AQ macrocycle were 4.3 and 5.8%, respectively (under a nitrogen atmosphere).

2.3. Electrode Preparation. A 3 mm diameter GC disc-type electrode (BASI) was used in all experiments as the working electrode (WE), and prior to use, it was polished for 30 s each with Buehler Micropolish II deagglomerated alumina with decreasing particle size from 1.0 to 0.3 and 0.05 μm. In between, the surface was rinsed with 18 MΩ water (MQ water) and isopropanol (VWR Chemicals) to remove excess alumina. To deposit nanotube samples onto the WE, SWCNT suspensions in isopropanol with a loading of 5.0 mg mL^{-1} were prepared and sonicated for 2 h prior to use. Then, 20 μL aliquots were drop-cast onto the glassy carbon WE and dried for 30 min under ambient conditions.

Platinum plates (Pt) were used as the counter electrode together with either commercially available Ag/AgCl (3 M KCl) (from BASI) reference electrodes (REs) in aqueous solutions or Ag/AgCl quasi-reference electrodes (QREs) in organic solutions for electrochemical investigations. In the case of the QRE, the calibration against the standard hydrogen electrode (SHE) was done by addition of ferrocene (Sigma Aldrich, >98%) and the determination of the position of this redox potential.

2.4. Electrochemical Experiments. All electrochemical measurements were performed on a Jaissle Potentiostat−Galvanostat PGU10V-100 mA. A three-electrode one-compartment (for organic solution) or two-compartment (for aqueous solution) electrochemical cell was used. The mentioned GC was employed as the WE. Platinum (Pt) plates were used as the counter electrode. In aqueous solution, a Ag/AgCl (3 M KCl) RE was used in the system, while in organic solutions, a Ag/AgCl QRE was used. The QRE was prepared by anodization in 1 M of HCl solution and the calibration against the SHE was performed by testing with ferrocene. Throughout this whole work, all potentials mentioned are referenced to the SHE.

For cyclic voltammetry (CV) experiments in organic solvents, 15 mL of acetonitrile (MeCN) (Roth, >99.9%) containing 0.1 M $TBAPF_6$ (Sigma Aldrich, >99.0%) was used as the electrolyte solution. In aqueous solution, CV experiments were done in 20 mL of 0.1 M Na_2SO_4 (Sigma Aldrich, >99.0%) or 0.1 M NaOH (Alfa Aesar) as the electrolyte solution. Before measurements under N_2-saturated conditions, the cell was purged with N_2 for 30 and 60 min for MeCN and aqueous solutions, respectively. In the case of O_2 saturation, the solutions were purged with O_2 (Linde Gas GmbH 5.0) for 30 min.

To prove the catalytic activities of AQ-MINT, AQ@SWCNTs, and SWCNTs toward the reduction of O_2 to H_2O_2, a constant potential at −0.33 V (chronoamperometry) was applied for 8 h under two conditions: neutral (0.1 M Na_2SO_4) and basic (0.1 M NaOH) aqueous solutions. Before applying the potential as well as during chronoamperometry, sample aliquots of 150 μL of the electrolyte solution were taken for H_2O_2 quantification. The H_2O_2 quantification was done following a previous report from Apaydin et al.[51] using a colorimetric detection method (see Supporting Information Figure S7 for further details).

For the rotating disc electrode (RDE) measurements, an IPS Rotator 2016 rotating unit with IPS PI-ControllerTouch and an IPS Jaissle PGU BI-1000 Bipotentiostat/Galvanostat were used. An 8 mm diameter GC disc in poly(chlorotrifluoroethylene) (PCTFE) was used as the WE and polished as mentioned above. A platinized electrode and Ag/AgCl (3 M KCl) (Messtechnik Meinsberg) were

https://dx.doi.org/10.1021/acsami.0c06516
ACS Appl. Mater. Interfaces 2020, 12, 32615−32621

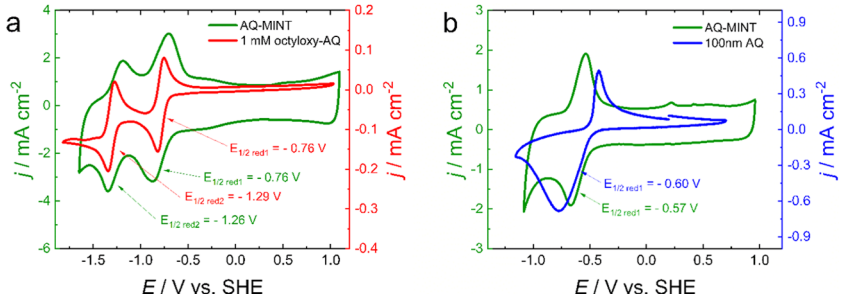

Figure 2. Cyclic voltammograms of (a) AQ-MINT (green line) and 1mM octyloxy-AQ (red line) in MeCN containing 0.1 M $TBAPF_6$ and (b) drop-cast AQ-MINT (green line) and a 100 nm thin film of AQ in 0.1 M Na_2SO_4 aqueous solution under N_2-saturated conditions at 20 mV s^{-1}.

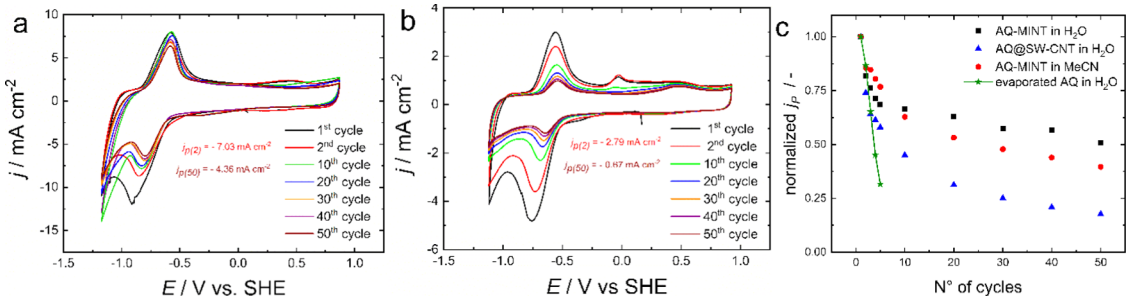

Figure 3. Cyclic voltammograms of (a) AQ-MINT and (b) AQ@SWCNTs in 0.1 M Na_2SO_4 upon 50 cycles. (c) Normalized peak current densities of the first reduction peak.

used as the counter and reference electrodes. To achieve comparable surface loading, 141 μL of the 5 mg mL^{-1} nanotube suspensions was drop-cast and dried prior to use.

3. RESULTS AND DISCUSSION

3.1. Spectroscopic Characterization. The absorption spectra of the SWCNTs (Figure S8) showed features in the S11 and S22 regions of the spectra with the absorption of the (6,5) nanotubes at 1002 and 576 nm. Upon functionalization through mechanical bonds, these bands were shifted to 999 and 576 nm, respectively. Regarding the supramolecular sample, we obtained the same values as those of the MINT sample, 999 and 576 nm.

The three Raman spectra (Figure S9) are very similar, thus proving that the structure of the nanotubes is preserved upon modification, with no increase in the relative intensity of the D band. All of these findings are in agreement with the noncovalent functionalization of the SWCNTs. Meanwhile, the G band is shifted from 1576 cm^{-1} in the pristine SWCNTs to 1584 cm^{-1} in AQ-MINT and 1586 cm^{-1} in AQ@SWCNTs. In addition, the D band is also shifted from 2600 cm^{-1} in the pristine SWCNTs to 2613 cm^{-1} in AQ-MINT and 2614 cm^{-1} in AQ@SWCNTs. This effect is due to the presence of the electron acceptor anthraquinone.[52]

In the PLE map spectra (Figure S10), the (6,5) SWNT configuration was detected. Upon the formation of AQ-MINT and AQ@SWCNTs, the (6,5) signal was totally quenched.

3.2. Electrochemical Stability Tests. The electrochemical behavior of AQ-MINT was investigated via cyclic voltammetry (CV) either in an organic solvent (acetonitrile, MeCN) or in aqueous solution as shown in Figure 2. For comparison with nonimmobilized AQ, a dissolved octyloxy-AQ derivative (Figure S11) and an evaporated film of pure AQ were studied. Figure 2a presents the electrochemical features of drop-cast AQ-MINT samples in MeCN and 1 mM dissolved octyloxy-AQ. Both cyclic voltammograms are comparable, except that a large capacitive current from the CNT carrier is observed in the case of the immobilized AQ-MINT (see Figure S12 for SWCNT CV curves). The graphs show two separated reversible one-electron reduction features of AQ at virtually identical $E_{1/2}$'s of −0.76 and −1.26/−1.29 V.[53] The electrochemical features of AQ-MINT and the evaporated thin film of AQ in aqueous solution are shown in Figure 2b. The graphs present one reversible and concerted two-electron reduction features. However, the reduction potential of AQ-MINT with $E_{1/2}$ = −0.57 V is 30 mV less negative and its peak separation (ΔE_P) is smaller, as compared to that of thin-film AQ. This smaller ΔE_P in the case of AQ-MINT together with the reported delamination of hydroquinone in the case of the evaporated AQ[54] shows that AQ-MINT offers a versatile redox system. This is in accordance with the literature[30] of adsorbed species on SWCNTs that stacking induces faster charge-transfer kinetics resulting in smaller ΔE_P.

The stability study of the immobilized AQ-MINT was performed with 50 CV cycles, as shown in Figure 3. The AQ@SWCNTs and the evaporated AQ film were investigated in a similar manner. Figure 3 shows that AQ-MINT is more stable due to a lower decrease in the reductive peak current as compared to the supramolecular form. This observation was strengthened by the comparison of the relative loss of the peak current density (j_P) upon 50 cycles. To determine j_P, the observed peak height was subtracted by a baseline. In the AQ-MINT case, j_P decreased by 38% from the 2nd to the 50th cycles, whereas in the AQ@SWCNT case, the loss roughly doubled by 76%. These decreases exponentially decayed while j_P of the evaporated AQ thin film decayed linearly by 68% within the first five cycles (Figure 3c). Cycle stability with comparable behavior was also observed in MeCN (Figure S13). According to the literature,[35] kinetic studies with CV at different scan rates were performed which showed, as expected for immobilized materials, a linear relation between the scan

https://dx.doi.org/10.1021/acsami.0c06516
ACS Appl. Mater. Interfaces 2020, 12, 32615−32621

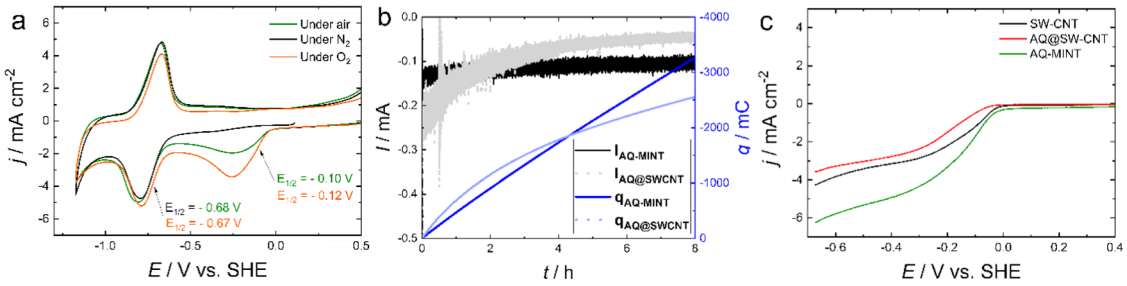

Figure 4. (a) Cyclic voltammograms of AQ-MINT in 0.1 M NaOH under air (green line), N_2 (black line), and O_2 (orange line) conditions. (b) Chronoamperograms and accumulated charges of AQ-MINT and AQ@SWCNTs at a constant potential of −0.33 V vs SHE in 0.1 M NaOH. (c) RDE-LSV results of AQ-MINT, AQ@SWCNTs, and SWCNTs in 0.1 M NaOH at a rotation speed of 1200 rpm.

rate (v) and j_P for both the AQ-MINT and the supramolecular sample (see Supporting Information Figure S14 for further details).

3.3. Electrochemical Oxygen Reduction. As AQ derivatives are known as chemical[22,52] as well as electrochemical[24,26,28] catalysts for the ORR to H_2O_2 vide supra, the AQ-MINT was investigated for its electrocatalytic activity under O_2-saturated conditions. AQ@SWCNTs and pristine SWCNTs were also tested as controls. Figure 4a shows that the characteristic AQ peak[55] at around −0.68 V is observed under all conditions. Upon O_2 saturation, a reduction broad peak around −0.10/−0.12 V as a result of oxygen reduction was observed. Starting from +0.50 V, some oxidative processes on the CNT occurred. Bare SWCNTs showed only the broad, capacitive current with a small reductive step upon O_2 reduction (Figure S12). To prove the catalytic activities of AQ-MINT, AQ@SWCNTs, and SWCNTs toward the reduction of O_2 to H_2O_2, a constant potential at −0.33 V was applied for 8 h under two conditions: neutral (0.1 M Na_2SO_4) and basic (0.1 M NaOH) aqueous solutions (see Supporting Information Table S1 for full details). The transient curves in Figure 4b showed that the current in the AQ-MINT case was stable over the 8 h period, whereas the AQ@SWCNT sample revealed a drastic decrease in current from −0.24 to −0.05 mA cm^{-2} within the 8 h reaction. This decrease was attributed to the delamination of the AQ electroactive species, which was in accordance with the cycle stability experiments in Figure 3b. Furthermore, the CV curves of AQ-MINT before and after the electrolysis showed nearly no difference in terms of electroactive AQ peaks, which supported the stable transient curve (Figure S15).

Table 1 reveals that basic conditions are more favorable for oxygen reduction, compared to neutral pH, which is in accordance with the literature.[52] In the case of AQ-MINT, the amount produced was increased from 1.9 μmol in neutral conditions to 7.0 μmol in alkaline conditions. As observed in control experiments, the pristine SWCNTs also showed a small catalytic effect, which was also already reported in the literature.[13,56] This effect might be attributed to traces of catalytically active metals or small defects as a result of the CNT production process,[13,57] as well as the intrinsic catalytic activity of GC.[58] However, both AQ modified samples presented enhanced catalytic activity over SWCNTs by a factor of 2 for AQ@SWCNTs and a factor of 3 for AQ-MINT. Considering the amount of AQ molecules in MINT and supramolecular cases, turnover numbers (TON) were calculated as reported in Table 1, which also substantiated the improved catalysis. Including the total mass of MINT and the activity from the supporting material, the average H_2O_2 production rate per mass was found to be 8.8 μmol mg^{-1} h^{-1} for AQ-MINT in basic aqueous solution. As outstanding reports, the direct synthesis from the elements on Pd nanoparticles[52] was achieved with a rate of 1100 μmol mg^{-1} $h^{-1}$and photoelectrocatalysis with epindolidione[21] was reported with a rate of 120 μmol mg^{-1} h^{-1}. Since the mass of CNTs was included in the total mass, the comparison of the rate per mass observed in each catalyst might slightly distort the performance of our systems.

Table 1. Comparison of the Total Amounts of H_2O_2 Produced over 8 h Electrolysis Reaction Time

	In 0.1 M Na_2SO_4		In 0.1 M NaOH	
	$n_{H_2O_2}$ in 8 h μmol^{-1}	TON	$n_{H_2O_2}$ in 8 h μmol^{-1}	TON
AQ-MINT	1.9	116	7.0	417
AQ@SWCNTs	1.4	75	4.4	236
SWCNTs	0.5		2.2	

To perform further electrocatalytic studies on the oxygen reduction process, RDE experiments were performed with SWCNTs, AQ@SWCNTs, and AQ-MINT at various rotation speeds. The goal was to obtain preliminary mechanistic insights by determination of the number of transferred electrons per process. Figure 4c shows an increase in current upon an increase in the rotational speed (ω), and the most pronounced behavior is observed for AQ-MINT. The Koutecki−Levich analysis revealed that upon drop-casting the samples, we substantially underestimated our electroactive electrode surface area by considering only the geometrical one. As this increase in the electrode surface area was related to the organization of the NTs on the surface, different ways of organization between the samples might be because of the attachments, which would be in accordance with the reorganization through hybridization reported by Lee et al.[30] Nevertheless, the intercepts of the Koutecki−Levich analysis revealed that among the as-cast films, AQ-MINT showed the highest i_K compared to SWCNTs and AQ@SWCNTs (Figure S16b).To prove this speculation of organization, advanced studies with higher resolution SEM facilities than we have would be necessary.

4. CONCLUSIONS

In this work, we explored the approach of interlocking the organic molecule AQ around carbon nanotubes (MINTs) for efficient immobilization. Such advanced noncovalent architectures could solve the problem of dissolution instability of physically adsorbed organic molecules upon electrochemical reduction. Besides the enhancement of stability while retaining

https://dx.doi.org/10.1021/acsami.0c06516
ACS Appl. Mater. Interfaces 2020, 12, 32615−32621

the electrochemical properties of the pristine molecule, efficient immobilization toward electrochemistry could be demonstrated by a linear relation of j_P vs v plots. Furthermore, a proof of concept for the electrocatalytic application of AQ-MINT toward oxygen reduction was explored. In addition to the superior stability, an improvement in the H_2O_2 production rate in AQ-MINT systems revealed promising properties of MINTs as immobilization carriers. The promising results described herein reveal that there is still room for further investigations of different MINT-type materials for other catalytic applications.

■ ASSOCIATED CONTENT

Supporting Information

The Supporting Information is available free of charge at https://pubs.acs.org/doi/10.1021/acsami.0c06516.

Synthetic procedures, TGA−data, UV−vis absorption data, Raman data, H_2O_2 determination, additional electrochemical measurement graphs, tabulated results from H_2O_2 production experiments, and RDE results (PDF)

■ AUTHOR INFORMATION

Corresponding Authors

Emilio M. Pérez − *IMDEA Nanociencia, Ciudad Universitaria de Cantoblanco, 28049 Madrid, Spain;* orcid.org/0000-0002-8739-2777; Email: emilio.perez@imdea.org

Dong Ryeol Whang − *Linz Institute for Organic Solar Cells (LIOS), Institute of Physical Chemistry, Johannes Kepler University Linz, 4040 Linz, Austria; Department of Advanced Materials, Hannam University, Yuseong-Gu, Daejeon 34054, Republic of Korea;* orcid.org/0000-0001-8402-2140; Email: whang@hnu.kr

Authors

Dominik Wielend − *Linz Institute for Organic Solar Cells (LIOS), Institute of Physical Chemistry, Johannes Kepler University Linz, 4040 Linz, Austria*

Mariano Vera-Hidalgo − *IMDEA Nanociencia, Ciudad Universitaria de Cantoblanco, 28049 Madrid, Spain*

Hathaichanok Seelajaroen − *Linz Institute for Organic Solar Cells (LIOS), Institute of Physical Chemistry, Johannes Kepler University Linz, 4040 Linz, Austria;* orcid.org/0000-0002-1554-3644

Niyazi Serdar Sariciftci − *Linz Institute for Organic Solar Cells (LIOS), Institute of Physical Chemistry, Johannes Kepler University Linz, 4040 Linz, Austria;* orcid.org/0000-0003-4727-1193

Complete contact information is available at: https://pubs.acs.org/10.1021/acsami.0c06516

Author Contributions

‖D.W. and M.V.-H. contributed equally to this work.

Notes

The authors declare no competing financial interest.

■ ACKNOWLEDGMENTS

Funding from the European Union (ERC-Starting Grant: 307609 and Proof-of-Concept: 842606), MINECO (CTQ2017-86060-P), and the Comunidad de Madrid (Grant: MAD2D-CM program S2013/MIT-3007) is gratefully acknowledged. IMDEA Nanociencia acknowledges support from the "Severo Ochoa" Programme for Centres of Excellence in R&D (MINECO, Grant: SEV-2016-0686). The authors gratefully acknowledge financial support from the Austrian Science Foundation (FWF) through the Wittgenstein Prize for Prof. N.S.S. (Z222-N19). The authors also thank Dr. Dogukan Hazar Apaydin for the initial help regarding the H_2O_2 quantification method and evaporated AQ thin films.

■ REFERENCES

(1) Etacheri, V.; Marom, R.; Elazari, R.; Salitra, G.; Aurbach, D. Environmental Science Challenges in the Development of Advanced Li-Ion Batteries: A Review. *Energy Environ. Sci.* **2011**, *4*, 3243−3262.

(2) Häupler, B.; Wild, A.; Schubert, U. S. Carbonyls: Powerful Organic Materials for Secondary Batteries. *Adv. Energy Mater.* **2015**, *5*, No. 1402034.

(3) Alotto, P.; Guarnieri, M.; Moro, F. Redox Flow Batteries for the Storage of Renewable Energy: A Review. *Renewable Sustainable Energy Rev.* **2014**, *29*, 325−335.

(4) González, A.; Goikolea, E.; Andoni, J.; Mysyk, R. Review on Supercapacitors: Technologies and Materials. *Renew. Sustain. Energy Rev.* **2016**, *58*, 1189−1206.

(5) Dalle, K. E.; Warnan, J.; Leung, J. J.; Reuillard, B.; Karmel, I. S.; Reisner, E. Electro- and Solar-Driven Fuel Synthesis with First Row Transition Metal Complexes. *Chem. Rev.* **2019**, *119*, 2752−2875.

(6) Eftekhari, A. Electrocatalysts for Hydrogen Evolution Reaction. *Int. J. Hydrogen Energy* **2017**, *42*, 11053−11077.

(7) Aresta, M. In *Carbon Dioxide Recovery and Utilization*; Aresta, M., Ed.; Springer Science+Business Media: Dordrecht, 2003.

(8) Aresta, M. In *Carbon Dioxide as Chemical Feedstock*; Aresta, M., Ed.; WILEY-VCH Verlag GmbH & Co. KGaA: Weinheim, 2010.

(9) Benson, E. E.; Kubiak, C. P.; Sathrum, A. J.; Smieja, J. M. Electrocatalytic and Homogeneous Approaches to Conversion of CO2 to Liquid Fuels. *Chem. Soc. Rev.* **2009**, *38*, 89−99.

(10) Nocera, D. G. The Artificial Leaf. *Acc. Chem. Res.* **2012**, *45*, 767−776.

(11) Berardi, S.; Drouet, S.; Francàs, L.; Gimbert-Suriñach, C.; Guttentag, M.; Richmond, C.; Stoll, T.; Llobet, A. Molecular Artificial Photosynthesis. *Chem. Soc. Rev.* **2014**, *43*, 7501−7519.

(12) Francke, R.; Schille, B.; Roemelt, M. Homogeneously Catalyzed Electroreduction of Carbon Dioxide - Methods, Mechanisms, and Catalysts. *Chem. Rev.* **2018**, *118*, 4631−4701.

(13) Dai, L.; Xue, Y.; Qu, L.; Choi, H.-J.; Baek, J.-B. Metal-Free Catalysts for Oxygen Reduction Reaction. *Chem. Rev.* **2015**, *115*, 4823−4892.

(14) Martinez, U.; Komini Babu, S.; Holby, E. F.; Zelenay, P. Durability Challenges and Perspective in the Development of PGM-Free Electrocatalysts for the Oxygen Reduction Reaction. *Curr. Opin. Electrochem.* **2018**, *9*, 224−232.

(15) Fukuzumi, S. Artificial Photosynthesis for Production of Hydrogen Peroxide and Its Fuel Cells. *Biochim. Biophys. Acta, Bioenerg.* **2016**, *1857*, 604−611.

(16) Rosser, T. E.; Gross, M. A.; Lai, Y.-H.; Reisner, E. Precious-Metal Free Photoelectrochemical Water Splitting with Immobilised Molecular Ni and Fe Redox Catalysts. *Chem. Sci.* **2016**, *7*, 4024−4035.

(17) Hammouche, M.; Lexa, D.; Savéant, J. M.; Momenteau, M. Catalysis of the Electrochemical Reduction of Carbon Dioxide by Iron("0") Porphyrins. *J. Electroanal. Chem. Interfacial Electrochem.* **1988**, *249*, 347−351.

(18) Steinlechner, C.; Roesel, A. F.; Oberem, E.; Päpke, A.; Rockstroh, N.; Gloaguen, F.; Lochbrunner, S.; Ludwig, R.; Spannenberg, A.; Junge, H.; Francke, R.; Beller, M. Selective Earth-Abundant System for CO 2 Reduction: Comparing Photo- and Electrocatalytic Processes. *ACS Catal.* **2019**, *9*, 2091−2100.

(19) Coskun, H.; Aljabour, A.; De Luna, P.; Farka, D.; Greunz, T.; Stifter, D.; Kus, M.; Zheng, X.; Liu, M.; Hassel, A. W.; Schöfberger, W.; Sargent, E. H.; Sariciftci, N. S.; Stadler, P. Biofunctionalized

Conductive Polymers Enable Efficient CO2 Electroreduction. *Sci. Adv.* **2017**, *3*, No. e1700686.
(20) Dey, S.; Mondal, B.; Chatterjee, S.; Rana, A.; Amanullah, S.; Dey, A. Molecular Electrocatalysts for the Oxygen Reduction Reaction. *Nat. Rev. Chem.* **2017**, *1*, No. 0098.
(21) Jakešová, M.; Apaydin, D. H.; Sytnyk, M.; Oppelt, K. T.; Heiss, W.; Sariciftci, N. S.; Głowacki, E. D. Hydrogen-Bonded Organic Semiconductors as Stable Photoelectrocatalysts for Efficient Hydrogen Peroxide Photosynthesis. *Adv. Funct. Mater.* **2016**, *26*, 5248−5254.
(22) Goor, G.; Glenneberg, J.; Jacobi, S. Hydrogen Proxide. *Ullmann's Encycl. Ind. Chem.* **2012**, *18*, 393−427.
(23) Mirkhalaf, F.; Tammeveski, K.; Schiffrin, D. J. Substituent Effects on the Electrocatalytic Reduction of Oxygen on Quinone-Modified Glassy Carbon Electrodes. *Phys. Chem. Chem. Phys.* **2004**, *6*, 1321−1327.
(24) Sarapuu, A.; Helstein, K.; Vaik, K.; Schiffrin, D. J.; Tammeveski, K. Electrocatalysis of Oxygen Reduction by Quinones Adsorbed on Highly Oriented Pyrolytic Graphite Electrodes. *Electrochim. Acta* **2010**, *55*, 6376−6382.
(25) Tammeveski, K.; Kontturi, K.; Nichols, R. J.; Potter, R. J.; Schiffrin, D. J. Surface Redox Catalysis for O2 Reduction on Quinone-Modified Glassy Carbon Electrodes. *J. Electroanal. Chem.* **2001**, *515*, 101−112.
(26) Vaik, K.; Mäeorg, U.; Maschion, F. C.; Maia, G.; Schiffrin, D. J.; Tammeveski, K. Electrocatalytic Oxygen Reduction on Glassy Carbon Grafted with Anthraquinone by Anodic Oxidation of a Carboxylate Substituent. *Electrochim. Acta* **2005**, *50*, 5126−5131.
(27) Hoang, P. M.; Holdcroft, S.; Funt, B. L. Preparation and Properties of Electrodes Modified by Polymeric Films with Pendant Anthraquinone Groups. *J. Electrochem. Soc.* **1985**, *132*, 2129−2133.
(28) Mooste, M.; Kibena-Põldsepp, E.; Matisen, L.; Tammeveski, K. Oxygen Reduction on Anthraquinone Diazonium Compound Derivatised Multi-Walled Carbon Nanotube and Graphene Based Electrodes. *Electroanalysis* **2017**, *29*, 548−558.
(29) Werner, D.; Apaydin, D. H.; Portenkirchner, E. An Anthraquinone / Carbon Fiber Composite as Cathode Material for Rechargeable Sodium-Ion Batteries. *Batteries Supercaps* **2018**, *1*, 160−168.
(30) Lee, M.; Hong, J.; Kim, H.; Lim, H.; Cho, S. B.; Kang, K.; Park, C. B. Organic Nanohybrids for Fast and Sustainable Energy Storage. *Adv. Mater.* **2014**, *26*, 2558−2565.
(31) Bourourou, M.; Elouarzaki, K.; Lalaoui, N.; Agnès, C.; Le Goff, A.; Holzinger, M.; Maaref, A.; Cosnier, S. Supramolecular Immobilization of Laccase on Carbon Nanotube Electrodes Functionalized with (Methylpyrenylaminomethyl)Anthraquinone for Direct Electron Reduction of Oxygen. *Chem. - Eur. J.* **2013**, *19*, 9371−9375.
(32) Dai, H. Carbon Nanotubes: Synthesis, Integration, and Properties. *Acc. Chem. Res.* **2002**, *35*, 1035−1044.
(33) Weigl, S.; Bretterbauer, K.; Hesser, G.; Schöfberger, W.; Paulik, C. Synthesis, Characterization, and Description of Influences on the Stabilizing Activity of Antioxidant-Functionalized Multi-Walled Carbon Nanotubes. *Carbon* **2015**, *81*, 305−213.
(34) Lamprecht, C.; Huzil, J. T.; Ivanova, M. V.; Foldvari, M. Non-Covalent Functionalization of Carbon Nanotubes with Surfactants for Pharmaceutical Applications - A Critical Mini-Review. *Drug Delivery Lett.* **2011**, *1*, 45−57.
(35) Gong, Z.; Zhang, G.; Wang, S. Electrochemical Reduction of Oxygen on Anthraquinone/Carbon Nanotubes Nanohybrid Modifed Glassy Carbon Electrode in Neutral Medium. *J. Chem.* **2013**, *2013*, 1−9.
(36) Belin, T.; Epron, F. Characterization Methods of Carbon Nanotubes: A Review. *Mater. Sci. Eng., B* **2005**, *119*, 105−118.
(37) Zhang, W.; Shaikh, A. U.; Tsui, E. Y.; Swager, T. M. Cobalt Porphyrin Functionalized Carbon Nanotubes for Oxygen Reduction. *Chem. Mater.* **2009**, *21*, 3234−3241.
(38) De Juan, A.; Pouillon, Y.; Ruiz-González, L.; Torres-Pardo, A.; Casado, S.; Martín, N.; Rubio, Á.; Pérez, E. M. Mechanically Interlocked Single-Wall Carbon Nanotubes. *Angew. Chem., Int. Ed.* **2014**, *53*, 5394−5400.
(39) Pérez, E. M. Putting Rings around Carbon Nanotubes. *Chem. - Eur. J.* **2017**, *23*, 12681−12689.
(40) Mena-Hernando, S.; Pérez, E. M. Mechanically Interlocked Materials. Rotaxanes and Catenanes beyond the Small Molecule. *Chem. Soc. Rev.* **2019**, *48*, 5016−5032.
(41) Blanco, M.; Nieto-Ortega, B.; De Juan, A.; Vera-Hidalgo, M.; López-Moreno, A.; Casado, S.; González, L. R.; Sawada, H.; González-Calbet, J. M.; Pérez, E. M. Positive and Negative Regulation of Carbon Nanotube Catalysts through Encapsulation within Macrocycles. *Nat. Commun.* **2018**, *9*, No. 2671.
(42) Huang, F.; Anslyn, E. V. Introduction: Supramolecular Chemistry. *Chem. Rev.* **2015**, *115*, 6999−7000.
(43) Amabilino, D. B.; Gale, P. A. Supramolecular Chemistry Anniversary. *Chem. Soc. Rev.* **2017**, *46*, 2376−2377.
(44) Kassem, S.; Van Leeuwen, T.; Lubbe, A. S.; Wilson, M. R.; Feringa, B. L.; Leigh, D. A. Artificial Molecular Motors. *Chem. Soc. Rev.* **2017**, *46*, 2592−2621.
(45) Liu, Z.; Nalluri, S. K. M.; Stoddart, J. F. Surveying Macrocyclic Chemistry: From Flexible Crown Ethers to Rigid Cyclophanes. *Chem. Soc. Rev.* **2017**, *46*, 2459−2478.
(46) Reuillard, B.; Ly, K. H.; Rosser, T. E.; Kuehnel, M. F.; Zebger, I.; Reisner, E. Tuning Product Selectivity for Aqueous CO2 Reduction with a Mn(Bipyridine)-Pyrene Catalyst Immobilized on a Carbon Nanotube Electrode. *J. Am. Chem. Soc.* **2017**, *139*, 14425−14435.
(47) Aoi, S.; Mase, K.; Ohkubo, K.; Fukuzumi, S. Selective Electrochemical Reduction of CO2 to CO with a Cobalt Chlorin Complex Adsorbed on Multi-Walled Carbon Nanotubes in Water. *Chem. Commun.* **2015**, *51*, 10226−10228.
(48) Canevet, D.; Gallego, M.; Isla, H.; Juan, A.; De; Emilio, M. P. Macrocyclic Hosts for Fullerenes: Extreme Changes in Binding Abilities with Small Structural Variations. *J. Am. Chem. Soc.* **2011**, *133*, 3184−3190.
(49) López-Moreno, A.; Pérez, E. M. Pyrene-Based Mechanically Interlocked SWNTs. *Chem. Commun.* **2015**, *51*, 5421−5424.
(50) de Juan-Fernández, L.; Münich, P. W.; Puthiyedath, A.; Nieto-Ortega, B.; Casado, S.; Ruiz-González, L.; Pérez, E. M.; Guldi, D. M. Interfacing Porphyrins and Carbon Nanotubes through Mechanical Links. *Chem. Sci.* **2018**, *9*, 6779−6784.
(51) Apaydin, D. H.; Seelajaroen, H.; Pengsakul, O.; Thamyongkit, P.; Sariciftci, N. S.; Kunze-Liebhäuser, J.; Portenkirchner, E. Photoelectrocatalytic Synthesis of Hydrogen Peroxide by Molecular Copper-Porphyrin Supported on Titanium Dioxide Nanotubes. *ChemCatChem* **2018**, *10*, 1793−1797.
(52) Campos-Martin, J. M.; Blanco-Brieva, G.; Fierro, J. L. G. Hydrogen Peroxide Synthesis: An Outlook beyond the Anthraquinone Process. *Angew. Chem., Int. Ed.* **2006**, *45*, 6962−6984.
(53) Babaei, A.; Connor, P. A.; McQuillan, A. J.; Umapathy, S. UV-Visible Spectrooelectrochemistry of the Reduction Products of Anthraquinone in Dimethylformamide Solutions: An Advanced Undergraduate Experiment. *J. Chem. Educ.* **1997**, *74*, 1200.
(54) Wielend, D.; Apaydin, D. H.; Sariciftci, N. S. Anthraquinone Thin-Film Electrodes for Reversible CO2 Capture and Release. *J. Mater. Chem. A* **2018**, *6*, 15095−15101.
(55) Revenga, J.; Rodríguez, F.; Tijero, J. Study of the Redox Behavior of Anthraquinone in Aqueous Medium. *J. Electrochem. Soc.* **1994**, *141*, 330.
(56) Qu, J.; Shen, Y.; Qu, X.; Dong, S. Electrocatalytic Reduction of Oxygen at Multi-Walled Carbon Nanotubes and Cobalt Porphyrin Modified Glassy Carbon. *Electroanalysis* **2004**, *16*, 1444−1450.
(57) Kruusenberg, I.; Alexeyeva, N.; Tammeveski, K.; Kozlova, J.; Matisen, L.; Sammelselg, V.; Solla-Gullón, J.; Feliu, J. M. Effect of Purification of Carbon Nanotubes on Their Electrocatalytic Properties for Oxygen Reduction in Acid Solution. *Carbon* **2011**, *49*, 4031−4039.

https://dx.doi.org/10.1021/acsami.0c06516
ACS Appl. Mater. Interfaces 2020, 12, 32615−32621

(58) Šljukić, B.; Banks, C. E.; Compton, R. G. An Overview of the Electrochemical Reduction of Oxygen at Carbon-Based Modified Electrodes. *J. Iran. Chem. Soc.* **2005**, *2*, 1−25.

https://dx.doi.org/10.1021/acsami.0c06516
ACS Appl. Mater. Interfaces 2020, 12, 32615−32621